PHYSICAL REVIEW C **80**, 051001(R) (2009)

Interaction current in $pp \to pp\gamma$

K. Nakayama[1,2,*] and H. Haberzettl[3,†]

[1]*Department of Physics and Astronomy, University of Georgia, Athens, Georgia 30602, USA*

[2]*Institut für Kernphysik and Jülich Center for Hadron Physics, Forschungszentrum Jülich, D-52425 Jülich, Germany*

[3]*Center for Nuclear Studies, Department of Physics, The George Washington University, Washington, DC 20052, USA*

(Received 2 October 2009; published 11 November 2009)

The nucleon-nucleon bremsstrahlung reaction is investigated based on a fully gauge-invariant relativistic meson-exchange model approach. To account consistently for the complicated part of the interaction current (which at present is too demanding to be calculated explicitly), a generalized contact current is introduced following the approach of H. Haberzettl, K. Nakayama, and S. Krewald [Phys. Rev. C **74**, 045202 (2006)]. The contact interaction current is constructed phenomenologically such that the resulting full bremsstrahlung amplitude satisfies the generalized Ward-Takahashi identity. The formalism is applied to describe the high-precision proton-proton bremsstrahlung data at 190 MeV obtained at KVI [H. Huisman *et al.*, Phys. Rev. C **65**, 031001(R) (2002)]. The present results show good agreement with the data, thus removing the long-standing discrepancy between the theoretical predictions and experimental data. The present investigation, therefore, points to the importance of properly taking into account the interaction current for this reaction.

DOI: 10.1103/PhysRevC.80.051001 PACS number(s): 25.10.+s, 25.40.−h, 25.20.Lj, 13.75.Cs

The nucleon-nucleon (NN) bremsstrahlung reaction had been studied extensively in the past mainly to learn about off-shell properties of the NN interaction. It should be clear, however, that off-shell effects are model-dependent and therefore are meaningless quantities for comparison. In fact, Fearing and Scherer [1] have shown explicitly for NN bremsstrahlung and related processes that in field theories off-shell effects cannot be measured.

Even though the original motivation for investigating the NN bremsstrahlung reaction has fallen away, understanding the dynamics of the NN bremsstrahlung reaction, nevertheless, is of extreme importance in general for it is one of the most fundamental processes involving both electromagnetic and hadronic interactions. Its importance is all the more emphasized by the fact that, so far, none of the existing models of NN bremsstrahlung can describe the high-precision proton-proton bremsstrahlung data from KVI [2,3] for coplanar geometries involving small proton scattering angles. This is illustrated in Figs. 1(a) and 1(b), where the KVI data [2] for cross sections and analyzing powers are compared to the results of the microscopic calculations of Martinus, Scholten, and Tjon [4] and of Herrmann *et al.* [5]. Also shown in Fig. 1 are the TRIUMF data for the cross section [6]. As one can see, all the model calculations overestimate the measured cross sections, especially for asymmetric proton scattering angles ($\theta_1 \neq \theta_2$). In Ref. [2], some soft-photon model results are also compared with the data. In contrast to the microscopic models, these soft-photon models reproduce well the measured cross-section data. For the analyzing powers, however, it is the microscopic models that describe the data much better than the soft-photon models. (See also Ref. [7], where new data from KVI were reported sampling a part of phase space different from that for the earlier data [2,3]; the soft-photon models are found to be at odds with these new data.) It should be noted here that, strictly speaking, the kinematical regime of the KVI data for small proton scattering angles are outside of the range of applicability of Low's soft-photon theorem [8]. There are also a number of other microscopic model calculations available in the literature [9–15], which are dynamically similar to Refs. [4,5], addressing a variety of issues in the pp bremsstrahlung process.

A detailed discussion of the status of the discrepancy between the theoretical and the experimental results in pp bremsstrahlung can be found in Refs. [2,14,15]. This situation is extremely disturbing from a theoretical point of view, in particular, if one considers the fact that these data are obtained at a proton incident energy of only 190 MeV, well below the pion-production threshold energy of about 280 MeV. At such a low energy, one expects the nucleonic current to be dominating by far, and baryon resonances as well as meson-exchange currents should play only minimal roles in the reaction dynamics.

In this work we show that the interaction current mandated by gauge invariance plays a crucial role for this reaction and that its proper inclusion in theoretical models removes, to a large extent, the existing discrepancy between the theoretical and the experimental results. For direct and easy comparison, our present numerical results—explained later in this article—are shown in Figs. 1(c) and 1(d), directly below those shown in Figs. 1(a) and 1(b) obtained by other authors [4,5].

The present work uses a novel approach to describe the NN bremsstrahlung reaction. It is derived within a relativistic field-theory approach by coupling the photon everywhere possible in the underlying two-nucleon T matrix determined by the corresponding NN Bethe-Salpeter equation. The basic idea of this formalism is the same as what had been introduced by Haberzettl, Nakayama, and Krewald [16] for pion photoproduction, based on the field-theoretical approach of Haberzettl [17].

The full bremsstrahlung amplitude can be written as

$$M^\mu = (TG_0 + 1)J^\mu(1 + G_0T), \tag{1}$$

*nakayama@uga.edu

†helmut.haberzettl@gwu.edu

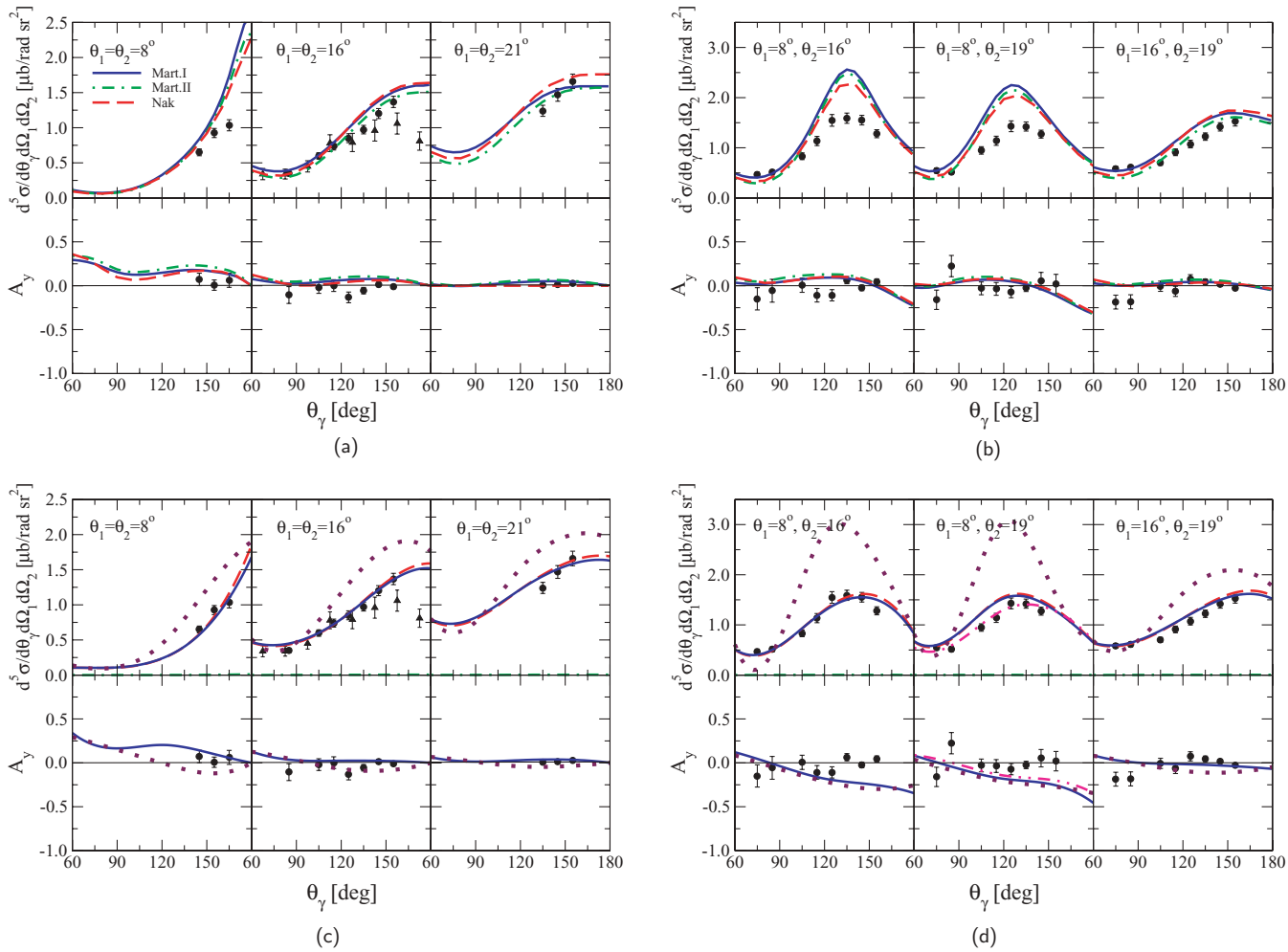

FIG. 1. (Color online) Comparison of the KVI data [2] (with corrected A_y sign [3]) for $pp \to pp\gamma$ in coplanar geometry at 190 MeV proton incident energy (circles) with various theoretical predictions. The TRIUMF data [6] for cross sections (triangles) are also displayed here. In each figure, the upper rows of panels display the cross sections and the lower rows the corresponding analyzing powers A_y for fixed proton scattering angles, θ_1 and θ_2, and as functions of the emitted photon angle, θ_γ, in the laboratory frame. The two figures on the left are for the symmetric proton scattering angles, $\theta_1 = \theta_2$, whereas the two figures on the right are for the asymmetric proton angles, $\theta_1 \neq \theta_2$. Panels (a) and (b) show the *results of previous model calculations*. The solid lines are the results of Ref. [4] including all the higher-order corrections; the dash-dotted lines pertain to the same model of Ref. [4] without the higher-order corrections. The dashed lines represent the results of Ref. [5]. Panels (c) and (d) show the same data arranged the same way compared to *results obtained with the present model*; that is, the theoretical results shown in panel (c) are to be compared to those of panel (a) and those of panel (d) are to be compared to those of panel (b). The dashed curves in panels (c) and (d) represent the nucleonic plus generalized contact current contributions; the dash-dotted curves correspond to the mesonic current, whereas the solid curves denote the total current contribution. Switching off the generalized four-point contact current (3) produces the dotted curves. The dashed-double-dotted lines for the middle section in panel (d) exhibit the parameter sensitivity explained in the text.

where the NNT matrices on the left and the right mediate the final-state interaction (FSI) and the initial-state interaction (ISI), respectively; G_0 denotes the intermediate propagation of two free nucleons. The current

$$J^\mu = d^\mu G_0 V + V G_0 d^\mu + V^\mu - V G_0 d^\mu G_0 V \qquad (2)$$

is the basic photon production current off the two nucleons composed, in general, of nucleonic, mesonic, and baryon-resonance currents, in addition to contact-type interaction currents, as shown in Fig. 2(a) for the example of single-meson exchanges. The two disconnected nucleonic contributions subsumed in d^μ are shown in Fig. 2(b); V is the NN interaction and V^μ describes the photon coupling to the internal mechanisms of the interaction V. We emphasize that the generic structures of Eqs. (1) and (2) are exact for any type of NN interaction. The proof follows straightforwardly from applying the "gauge derivative" procedure given in the Appendix of Ref. [17] to the connected part $G_0 T G_0$ of the NN Green's function. For NN interactions based on single-meson exchanges, the structure of J^μ depicted in Fig. 2 is complete. We draw particular attention to the contact-type currents appearing in the fourth and fifth term in Fig. 2(a). In general, they possess very complex internal dynamical structures that, at present, cannot be taken into account explicitly. However, they are constrained by gauge invariance. The corresponding constraint for the four-point current in the fourth diagram

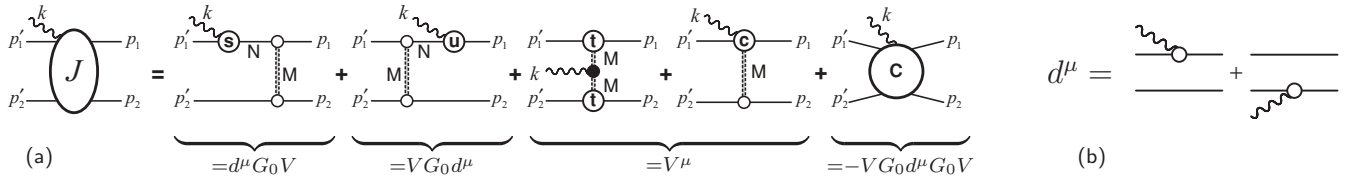

FIG. 2. (a) Basic production amplitude J^μ of Eq. (2) for $NN \to NN\gamma$ used in the present work. (Time proceeds from right to left.) The terms below the diagrams correspond to the respective ones in Eq. (2), with panel (b) showing the photon coupling to both intermediate nucleons subsumed in d^μ. The diagrams for the lower nucleon line analogous to diagrams 1, 2, and 4 are suppressed. N denotes the intermediate nucleon and M incorporates all exchanges of mesons π, η, ρ, ω, σ, and a_0 (former δ). In general, contributions to the NN interaction more complex than single-meson exchange may be considered as well. External legs are labeled by the four-momenta of the respective particles; the hadronic vertices s, u, and t (with the labels alluding to the corresponding Mandelstam variables) correspond to the same kinematic situations, respectively. The first two diagrams on the right-hand side describe the so-called nucleonic current and the meson-exchange current is depicted by the third diagram. The fourth diagram contains the $NM \to N\gamma$ four-point contact current of Eq. (3), labeled "c" in the diagram. The first four diagrams correspond to the *complete* gauge-invariant description for the process $NM \to N\gamma$ for the upper nucleon line. The last diagram (labeled "C") stands for the five-point contact-type current in general necessary to preserve gauge invariance of the entire amplitude, including the NN ISI and FSI contributions.

is based on the generalized Ward-Takahashi identity for the subprocess $NM \to N\gamma$.[1] By contrast, the five-point contact current depicted in the last diagram of Fig. 2(a) is constrained by demanding gauge invariance of the full bremsstrahlung process using the fact that the subprocesses already satisfy their respective gauge-invariance constraints.

For the current J^μ considered here shown in Fig. 2(a), in addition to the first two diagrams on the right-hand side with intermediate nucleons marked N, one may also consider contributions from intermediate baryon resonances. However, for the present application to the KVI data [2] at 190 MeV incident proton energy, we expect their contributions to be minimal, and we therefore have omitted such contributions.[2]

Our present approach is fully relativistic, employing a covariant three-dimensional reduction of the Bethe-Salpeter equation underlying the NN interaction [18]. As an immediate consequence of this reduction, one finds that the five-point contact current [last diagram in Fig. 2(a)] must not contribute to the four-divergence of the full amplitude; that is, it must be fully transverse. (This is *not* true for the amplitude M^μ evaluated in a full four-dimensional framework. The five-point contact current then is *essential* to maintaining gauge invariance.) In our present calculation, therefore, because it has no bearing on gauge invariance, we have dropped the five-point contact current entirely. Further details of the present formalism will be reported elsewhere.

In view of this finding, gauge-invariance constraints come to bear only on the four-point interaction current describing the $NM \to N\gamma$ subprocess in the fourth diagram of Fig. 2(a). To avoid having to deal with its very complex microscopic dynamical structures [16], we employ a generalized contact term that is constructed such that the resulting full amplitude satisfies the generalized Ward-Takahashi identity necessary to ensure full gauge invariance. The details of the contact term employed here are discussed later in this article in connection with Eq. (3). The only mesonic currents [cf. third diagram in Fig. 2(a)] contributing to pp bremsstrahlung are those arising from the anomalous couplings which cannot be obtained from coupling the photon to the underlying NN interaction. Following Ref. [16], we include the $\pi\rho\gamma$- and $\pi\omega\gamma$-exchange contributions in the present work which are the dominant mesonic currents for pp bremsstrahlung.

In the present work, we use the OBEP-B version of the Bonn NN interaction with its parameters slightly readjusted to reproduce the low-energy pp scattering length [18] (see also Ref. [5]). This interaction contains only nucleon and meson degrees of freedom. The reason for choosing this interaction is that, apart from the phenomenological form factors at the nucleon-nucleon-meson (NNM) vertices, it is a fully microscopic meson-exchange model and, as such, the photon can be attached consistently and uniquely to every part of the NN interaction except, of course, to the form factors. The latter mechanism introduces necessarily an ambiguity in how the photon couples to this interacting system. As alluded to previously, we account for it through the generalized four-point contact current given below. We note once more that with such a simple explicit microscopic model of the NN interaction based on a three-dimensional reduction of the underlying Bethe-Salpeter equation, no five-point contact current is required to maintain gauge invariance; that is, all currents can be calculated explicitly, with the exception of the four-point contact current arising from the photon coupling to the NNM vertices, as pointed out. A five-point contact current may be necessary when one uses a more sophisticated NN interaction

[1] See the corresponding discussion in Ref. [16] for the case of pion photoproduction that exemplifies the structure of the four-point contact current appearing in the fourth diagram of Fig. 2(a). This case is relevant here because the dynamics of NN bremsstrahlung can be largely understood as a meson capture process where the captured meson originates from a spectator nucleon, as can be seen in the first four diagrams in Fig. 2(a).

[2] For the Δ, in particular, we point to the results of Ref. [4] shown in Figs. 1(a) and 1(b) with (solid curves) and without (dashed-dotted curves) higher-order effects, where the former includes the Δ as well as the mesonic current contributions. They show that the Δ would have only a minor effect in the low-energy regime investigated here. This therefore cannot affect our overall conclusions. At higher energies, effects of the Δ resonance have been investigated by de Jong *et al.* [10].

that includes two-nucleon irreducible contributions, as would be the case, for example, with interactions including explicit Δ degrees. For such interactions, and also for those based on purely phenomenological approaches where the underlying microscopic structures are not known, the introduction of a five-point contact current becomes an unavoidable procedure.

As alluded to in footnote 1, it is instructive to consider the present approach from a different point of view. Ignoring for the moment the complication of a possible five-point contact current, the basic photon production amplitude J^μ can be viewed as being obtained from the inverse of the photoproduction reaction, that is, a meson capture reaction, where the captured meson originates from a second nucleon that is a spectator to the capture reaction. In this picture, the nucleon-meson FSI is accounted for effectively by the four-point contact current. This is discussed in detail in Ref. [16]. In this sense, one may think of the full bremsstrahlung amplitude given by Eq. (1) as being constructed from the two basic building blocks, the respective amplitudes for the $NN \to NN$ and the $NM \to N\gamma$ reactions, analogous to the approach described in Ref. [19] for calculating the $NN \to NN\eta$ process. Of course, in this simplified picture one ignores complications arising from the identity of the nucleons.

For the details of the derivation of the generalized four-point contact current involving a pseudoscalar meson exchange, we refer to Ref. [16]. Here, the required extension—to account for the virtual nature of the incoming and outgoing nucleons and the exchanged meson at the four-point vertex—is accomplished following the work of Ref. [20]. Furthermore, in the present work, the generalized four-point contact current is extended to include also the scalar and vector meson exchanges. Schematically, suppressing all Lorentz indices, we have for the fourth diagram in Fig. 2(a)

$$J^\mu_{c_1} = \sum_M (f_{2t}\Gamma_2) i\Delta_M \left[e_M f_{1t} \Gamma^\mu_{c_1} + \Gamma_1 \tilde{C}^\mu_1 \right], \tag{3}$$

where the summation runs over the exchanged mesons between the interacting nucleons 1 and 2. Nucleon 2 (described by its phenomenological form factor f_{2t} and its Lorentz operator structure Γ_2) is here the spectator nucleon that supplies the meson (described by the propagator Δ_M) participating in the $NM \to N\gamma$ subprocess at the other vertex. The corresponding four-point interaction current is described by the expression in the square brackets here. The first term contains the phenomenological form factor f_{1t} and current operator $\Gamma^\mu_{c_1}$; that is, this describes the usual Kroll-Ruderman-type $NNM\gamma$ contact vertex. The second term contains the Lorentz operator Γ_1 for the NNM vertex of nucleon 1 and the contact current [16,17]

$$\begin{aligned} \tilde{C}^\mu_1 \equiv & -e'_1 \frac{(2p'_1 + k)^\mu}{(p'_1 + k)^2 - {p'_1}^2} (f_{1s} - \hat{F}_1) \\ & - e_1 \frac{(2p_1 - k)^\mu}{(p_1 - k)^2 - p_1^2} (f_{1u} - \hat{F}_1) \\ & - e_M \frac{(2q - k)^\mu}{(q - k)^2 - q^2} (f_{1t} - \hat{F}_1) \end{aligned} \tag{4}$$

that is necessary for the preservation of gauge invariance because the nucleons have structure described by form factors. The factors e'_1, e_1, and e_M stand for the combined charge-isospin operators of the nucleons and meson at the four-point vertex. The subtractions of $\hat{F}_1$ in Eq. (4) are necessary to render $\tilde{C}^\mu_1$ pole-free; $\hat{F}_1$ is a phenomenological function chosen here as

$$\hat{F}_1 = R_1 - h \frac{(R_1 - \delta_s f_{1s})(R_1 - \delta_u f_{1u})(R_1 - \delta_t f_{1t})}{R_1^2}, \tag{5}$$

which is manifestly crossing symmetric. For nonzero charges e_x, one has $\delta_x = 1$ and zero otherwise; f_{1x} denote the hadronic form factor for the specified kinematics $x = s, u, t$ [cf. Fig. 2(a)]; p'_1 and p_1 are the four-momenta at the four-point vertex of the outgoing and incoming nucleon, respectively; and q and k stand for the four-momenta of the exchanged meson M and the emitted photon, respectively. In Eq. (5),

$$R_1 = 1 + e^{-z/a}(f - 1), \tag{6}$$

with $z = [(1 - \delta_s f_{1s})(1 - \delta_u f_{1u})(1 - \delta_t f_{1t})]^2$, and $f = F({p'_1}^2, p_1^2, q^2)$ denotes the hadronic form factor with the momentum arguments as indicated. Of course, an expression similar to Eq. (3) exists for the photon emerging from the NNM vertex of nucleon 2. [The latter diagram is not shown in Fig. 2(a).]

The only free parameters of our model are the parameters h and a appearing in Eqs. (5) and (6) in the generalized four-point contact currents involving the scalar, pseudoscalar, and vector meson exchanges [cf. Fig. 2(a), fourth diagram]. In principle, these parameters may both be chosen independently for different exchanged mesons, in addition to being functions of momenta at the four-point vertex. In the present work, we take them to be constant and equal for all the exchanged mesons for the sake of simplicity. Their values of $h = 2.5$ and $a = 1000$ have been adjusted to reproduce the KVI cross section data [2]. All coupling constants and form factors at the hadronic vertices are consistent with the Bonn NN interaction [18] we use here for the FSI and the ISI. The only exception is the $NN\omega$ coupling constant, $g_{NN\omega}$, and the cutoff parameter, Λ_π, in the $NN\pi$ form factor entering in the mesonic current. Following the discussion in Ref. [21], we take $g_{NN\omega} = 10$ and $\Lambda_\pi = 900$ MeV. Also, following the work of Refs. [19,21], we employ a form factor for the off-shell nucleon in the basic photon production current, J^μ, with a cutoff parameter value of $\Lambda_N = 1000$ MeV.

In Figs. 1(c) and 1(d), we show the present results for the cross sections and analyzing power for the symmetric (left panels) and asymmetric (right panels) proton scattering angles. As one can see, we now reproduce well the cross-section data for both symmetric and asymmetric proton scattering angles (solid curves). The dotted curves correspond to the results when the generalized contact current is switched off. This illustrates the importance of taking into account the interaction current properly, a feature that has been ignored in all the earlier models. In fact, our results without the contact current are very similar to the ones obtained in earlier models, especially for asymmetric proton scattering angles [compare, in particular, the top-row panels in Figs. 1(a) and 1(b) with those in Figs. 1(c) and 1(d), respectively]. The contact current,

however, does not affect the analyzing power significantly and thus leaves room for further improvements.

To provide some idea about how sensitive the present results are to the fit parameters h and a, the dashed-double-dotted curves in the middle panels of Fig. 1(d), for $\theta_1 = 8^\circ, \theta_2 = 19^\circ$, correspond to $h = 3.0$ in Eq. (5). Note that the agreement with the data improves for both the cross section and the analyzing power. The calculated results are rather insensitive to the parameter a in Eq. (6) once it is in the correct order-of-magnitude range.

The Bonn NN interaction [18] used here does not incorporate Coulomb effects. To account for them, we repeated the calculation using instead the Paris NN interaction [22], which includes the Coulomb interaction fully as described in Ref. [5]. We obtain results practically the same as the ones shown in Figs. 1(c) and 1(d) if we readjust the parameter value h in Eq. (5) to $h = 2.0$. The only noticeable Coulomb effect is a downward bending of the cross section near $\theta_\gamma = 180^\circ$ in the $\theta_1 = \theta_2 = 8^\circ$ geometry, which is in agreement with earlier findings [5,9].

In summary, our present results essentially resolve the long-standing discrepancy between theoretical and experimental results in the pp bremsstrahlung reaction. The new feature of the present model responsible for bringing the theoretical results in line with the measured high-precision cross-section data from KVI [2] is a generalized four-point contact current that accounts for the interaction current in the $NM \to N\gamma$ subprocess and that is constructed in such a way that the resulting full bremsstrahlung amplitude obeys the Ward-Takahashi identity and thus is gauge invariant.

In view of its phenomenological nature we do not expect the particular contact current employed here to provide a definitive resolution of all problems in NN bremsstrahlung processes. Nevertheless, our present results show that the interaction current is a necessary ingredient for bremsstrahlung calculations that cannot be neglected.

This work is supported in part by FFE-COSY Grant 41788390.

[1] H. W. Fearing and S. Scherer, Phys. Rev. C **62**, 034003 (2000).
[2] H. Huisman *et al.*, Phys. Rev. C **65**, 031001(R) (2002).
[3] M. Mahjour-Shafiei *et al.*, Phys. Rev. C **70**, 024004 (2004).
[4] G. H. Martinus, O. Scholten, and J. A. Tjon, Phys. Lett. **B402**, 7 (1997); Phys. Rev. C **56**, 2945 (1997); **58**, 686 (1998).
[5] V. Herrmann, K. Nakayama, O. Scholten, and H. Arellano, Nucl. Phys. **A582**, 568 (1995).
[6] J. G. Rogers *et al.*, Phys. Rev. C **22**, 2512 (1980).
[7] M. Mahjour-Shafiei *et al.*, Eur. Phys. J. A **41**, 25 (2009).
[8] F. E. Low, Phys. Rev. **110**, 974 (1958).
[9] A. Katsogiannis and K. Amos, Phys. Rev. C **47**, 1376 (1993); A. Katsogiannis, K. Amos, M. Jetter, and H. V. von Geramb, *ibid.* **49**, 2342 (1994); M. Jetter, H. Freitag, and H. V. von Geramb, Phys. Scr. **48**, 229 (1993).
[10] V. Herrmann and K. Nakayama, Phys. Rev. C **45**, 1450 (1992); F. de Jong, K. Nakayama, V. Herrmann, and O. Scholten, Phys. Lett. **B333**, 1 (1994); F. de Jong, K. Nakayama, and T.-S. H. Lee, Phys. Rev. C **51**, 2334 (1995); F. de Jong and K. Nakayama, *ibid.* **52**, 2377 (1995).
[11] M. Jetter and H. W. Fearing, Phys. Rev. C **51**, 1666 (1995).
[12] J. A. Eden and M. F. Gari, Phys. Lett. **B347**, 187 (1995); Phys. Rev. C **53**, 1102 (1996).
[13] S. Kondratyuk, G. H. Martinus, and O. Scholten, Phys. Lett. **B418**, 20 (1998).
[14] M. D. Cozma, G. H. Martinus, O. Scholten, R. G. E. Timmermans, and J. A. Tjon, Phys. Rev. C **65**, 024001 (2002).
[15] M. D. Cozma, O. Scholten, R. G. E. Timmermans, and J. A. Tjon, Phys. Rev. C **68**, 044003 (2003).
[16] H. Haberzettl, K. Nakayama, and S. Krewald, Phys. Rev. C **74**, 045202 (2006).
[17] H. Haberzettl, Phys. Rev. C **56**, 2041 (1997).
[18] R. Machleidt, Adv. Nucl. Phys. **19**, 189 (1989); J. Haidenbauer (private communication); following J. Haidenbauer and K. Holinde [Phys. Rev. C **40**, 2465 (1989)], the OBEP-B potential can be constrained to the low-energy scattering length with only a minor readjustment of its parameters.
[19] K. Nakayama, J. Speth, and T.-S. H. Lee, Phys. Rev. C **65**, 045210 (2002).
[20] K. Nakayama, Yongseok Oh, and H. Haberzettl, Phys. Rev. C **74**, 035205 (2006).
[21] K. Nakayama, A. Szczurek, C. Hanhart, J. Haidenbauer, and J. Speth, Phys. Rev. C **57**, 1580 (1998).
[22] M. Lacombe, B. Loiseau, J. M. Richard, R. Vinh Mau, J. Côté, P. Pirès, and R. de Tourreil, Phys. Rev. C **21**, 861 (1980).